

THE MATHEMATICAL THEORY OF FRONTOGENESIS

B. J. Hoskins

Department of Meteorology, University of Reading, Reading, England

1. INTRODUCTION

For over one hundred years it has been known that atmospheric depressions have cold frontal regions in which typically the temperature falls rapidly, the wind changes, and precipitation occurs. Sixty years ago Norwegian meteorologists shaped their polar front model in which depressions were considered to grow on a preexisting sloping thermal discontinuity; as the depressions grew it was considered that they distorted the discontinuity into a cold front and also a warm front. The dynamical view changed thirty years ago with the discovery by Charney (1947) and Eady (1949) that realistic depression structures may be obtained as the normal modes of the baroclinic instability of a smooth rather than discontinuous thermal contrast. Fronts then had to be viewed as being formed in a growing nonlinear baroclinic wave, though this secondary role in no way diminished their importance in practical meteorology. The theoretical interest shifted towards the mechanism for generating fronts, namely frontogenesis.

When upper air data became available in the 1950s it was apparent that strong frontal regions occurred in the upper troposphere as well as near the surface. Many studies (e.g. Reed & Danielsen 1959) suggested strongly that these upper air fronts are associated with the descent of a tongue of stratospheric air into the troposphere.

The existence of fronts in the ocean has been known for many years and when vertical sections were obtained (e.g. Voorhis & Hersey 1964 and Katz 1969) they suggested many structural similarities with atmospheric fronts. Further, the experimental work of Fultz (1952) and Faller (1956) has shown that fronts can be reproduced in laboratory experiments using differentially heated rotating water. Thus we conclude that details of latent-heat release and other diabatic heating, and of the boundary layer

and turbulent friction, are probably not crucial in the process of frontogenesis though they will clearly have important modifying effects in any particular case, and will be crucial in any steady-state front. The adiabatic, frictionless equations will be the basis of the work reviewed in this paper.

It is probably a mistake to attempt a rigorous definition of a front. However, in order to make it clear that the subject of this review is not the sea-breeze front, inter-tropical convergence zone, etc., some definition is required. A front is considered to be a region whose length scale is comparable with the radius of deformation (NH/f where N is a buoyancy frequency, H a relevant height scale, and f the Coriolis parameter) in one direction but much less than this in the cross direction, and across which there are significant changes in buoyancy and velocity with gradients tending to become very large in a finite time. The rotation of the fluid is crucial to the existence of the front.

2. ADVECTION OF A PASSIVE SCALAR

Although much of the interesting theory concerning frontogenesis is concerned with nonlinear feedback, it is helpful to begin by considering the advection of a passive scalar b , later taken to be the buoyancy, by a horizontal two-dimensional, nondivergent flow ($u, v, 0$):

$$Db/Dt = b_t + ub_x + vb_y = 0. \quad (1)$$

A usual way of discussing the rate of change of the gradient of b moving with the fluid (e.g. Mudrick 1974) is by introducing the deformation D with the stretching oriented along the dilatation axis. Then the so-called frontogenesis function (Miller 1948) is

$$\frac{D}{Dt} |\nabla b|^2 = D |\nabla b|^2 \cos 2\phi, \quad (2)$$

where ϕ is the angle between the dilatation axis and the b contour. If this angle is of magnitude $\pi/4$ or less, gradients in b grow following a fluid particle.

More information can often be obtained from a slightly different approach. Suppose that we are interested in the x gradient of b . Then (1) gives

$$\frac{D}{Dt} b_x = Q_1, \quad (3)$$

where

$$Q_1 = -u_x b_x - v_x b_y = -\partial(v, b)/\partial(x, y). \quad (4)$$

The x gradient of b on a fluid particle increases in time if the y component of wind increases along a b contour, moving with larger b on the right.

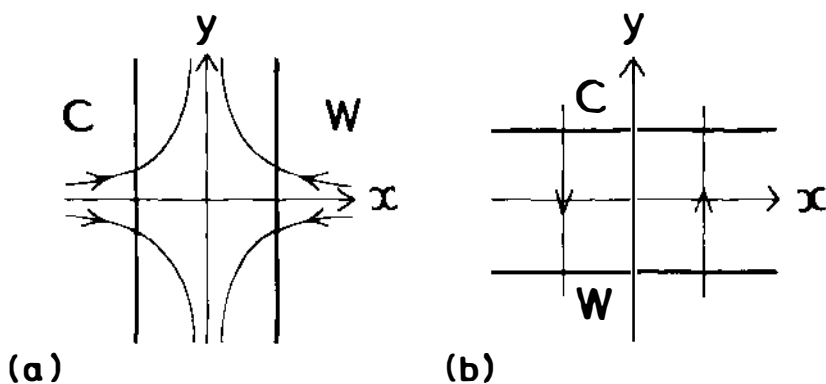


Figure 1 Mechanisms for forming an x gradient in buoyancy. Buoyancy contours are indicated by thick lines and light (warm) and heavy (cold) fluid are indicated by W and C respectively. Streamlines are shown by thin lines with arrows. (a) relies on horizontal convergence and (b) on horizontal shear.

Two simple cases have been discussed in many frontogenesis papers. Bergeron (1928) postulated that frontogenesis could occur in a simple deformation field $u = -\alpha x$, $v = \alpha y$. The case of b independent of y is shown in Figure 1a. The other component of the Jacobian is highlighted in the shear model investigated numerically by Williams (1967). A simple example is indicated in Figure 1b.

The vector form of (3) may be written

$$\frac{D}{Dt} \nabla b = \mathbf{Q}, \quad (5)$$

where $\mathbf{Q} = - \left(\mathbf{k} \wedge \frac{\partial \mathbf{v}}{\partial s} \right) \left| \frac{\partial b}{\partial n} \right|$, s and n being coordinates tangential and normal to b contours with n increasing in the direction of decreasing b . From (5) the "frontogenesis function" given in (2) has the alternative form $2\mathbf{Q} \cdot \nabla b$.

3. QUASI-GEOSTROPHIC FRONTOGENESIS

For a first look at the interaction of the changing buoyancy¹ and velocity fields we consider the small Rossby number approximation of quasi-geostrophic theory (for a detailed discussion of this theory, see, for example, Pedlosky 1979). The y momentum and buoyancy equations for a quasi-

¹In meteorological parlance, following Hoskins & Bretherton (1972), b can be taken to be g times potential temperature divided by a standard temperature.

geostrophic Boussinesq fluid in a coordinate system rotating with angular velocity $f/2$ about a vertical axis may be written

$$D_g v_g + f u_a = 0, \quad (6)$$

and

$$D_g b + N^2 w = 0, \quad (7)$$

where the geostrophic wind is $(u_g, v_g) = (-f^{-1} \phi_y, f^{-1} \phi_x)$, $u_a = u - u_g$ is the ageostrophic flow in the x direction, $b = \phi_z$, D_g is the time derivative moving with the geostrophic velocity, and $N(z)$ is the buoyancy frequency. v_g and b are linked by the "thermal wind" relation

$$f v_{gz} = b_x. \quad (8)$$

Rather as in the previous section, an x derivative of (7) gives

$$D_g b_x = Q_1 - N^2 w_x, \quad (9)$$

where Q_1 is given by (4) evaluated using geostrophic velocities. A z derivative of (6) shows, after a little manipulation, that we also have

$$D_g f v_{gz} = -Q_1 - f^2 u_{az}. \quad (10)$$

Equations (9) and (10) describe how the geostrophic velocity field acting through the term Q_1 attempts to destroy thermal wind balance (8) by changing the two parts by equal but opposite amounts. The role of the ageostrophic motion (u_a, w) is to maintain thermal wind balance. Subtracting (9) and (10) gives an equation for the ageostrophic motion in the x, z plane:

$$N^2 w_x - f^2 u_{az} = -2Q_1. \quad (11)$$

Geostrophic motion is nondivergent so that, if the y component of ageostrophic motion is independent of y , we may introduce a stream function ψ for the ageostrophic motion such that $(u_a, w) = (-\psi_z, \psi_x)$. From (11) the equation for ψ is

$$N^2 \psi_{xx} + f^2 \psi_{zz} = -2Q_1. \quad (12)$$

Using these ideas, we are able to obtain valuable insights into the dynamics of frontogenesis. Consider the frontogenetic situation shown in

Figure 2. There is a positive x gradient in b in balance with a positive vertical shear in v_g . Suppose that the large-scale geostrophic motion is tending to increase b_x everywhere, i.e. $Q_1 > 0$. In Figure 2 this is accomplished by large-scale convergence. As discussed above, the geostrophic motion must imply a tendency to decrease v_g , through the appearance of $-Q_1$ in (10). Thermal wind balance is maintained by the ageostrophic motion with w_x positive and u_{az} negative. The upward motion at positive x and downward motion at negative x act to decrease and increase b , respectively, thereby decreasing b_x . The negative u_a at upper levels and positive u_a at lower levels act to increase and decrease v_g , respectively, thereby increasing v_{gz} .

The stream-function equation (12) and the arguments from it are essentially simpler quasi-geostrophic forms of those given by Sawyer (1956) and Eliassen (1959, 1962). The more complete theory will be discussed in the next section.

Stone (1966), Williams & Plotkin (1968), and Williams (1968) used quasi-geostrophic theory to investigate the simple deformation model of frontogenesis. Their solutions exhibited the growth in gradients especially near boundaries. Away from horizontal boundaries the ageostrophic motion stopped the horizontal length scale of the b field from decreasing below the Rossby radius of deformation NH/f (H is the depth of fluid). On the boundaries w is zero and the scale decreases as dictated by the imposed field. The largest gradients in b occur in a vertical region and positive and negative vorticity exhibit equal growth. Many of these unrealistic features are easily traced to the omission of certain feedbacks in

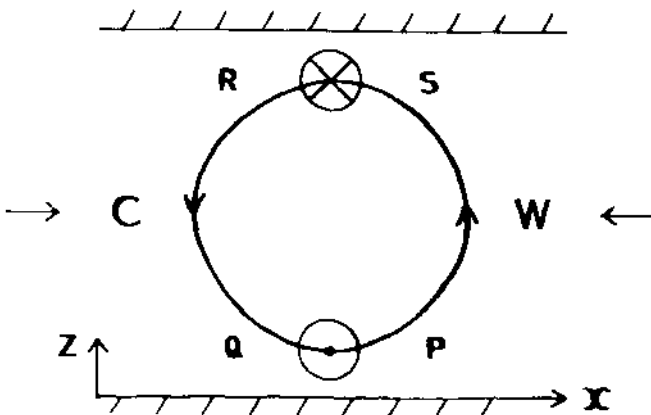


Figure 2 A frontogenetic situation in which a buoyancy gradient from heavy (C) to light (W) in thermal wind balance with a flow into the section at the top (⊗) and out of it at the bottom (⊙) is being increased by a large scale convergence in x indicated by arrows. The resulting ageostrophic cross-frontal circulation is shown by an arrowed streamline.

quasi-geostrophic theory. However, the qualitative effect of some of these feedbacks can be deduced from the quasi-geostrophic results. For example, consider the region P at the ground on the "warm" side of the temperature contrast. The ageostrophic velocity is clearly convergent ($u_{ax} < 0$) there and would, if included, imply the generation of larger gradients in b . Also at P the positive vorticity generation is underestimated because the nonlinear term (ξw_z) in the vorticity (ξ) equation

$$D\xi/Dt = (f + \xi)w_z \quad (13)$$

is not included. These arguments also apply to point R on the cold side at upper levels. However, at points Q and S the ageostrophic divergence would imply weaker gradients in b , and the neglected nonlinear term would imply smaller negative vorticity.

Quasi-geostrophic theory thus correctly suggests, though its solutions do not include, the formation of strong surface fronts with positive vorticity on the warm side of the buoyancy contrast, and that the region of maximum gradients slopes in the vertical from P to R . It highlights the role of horizontal boundaries in nonlinear frontogenesis. In the free atmosphere the ageostrophic circulation acts to inhibit the formation of large gradients. The final point to be made is that, unless the ageostrophic convergence at P increases as the local gradients increase, the vorticity [from (11)] and the gradients in b can only increase exponentially with time. Quasi-geostrophic theory does not even suggest the formation of frontal discontinuities in a finite time.

4. TWO-DIMENSIONAL SEMI-GEOSTROPHIC FRONTOGENESIS

Introduction

To produce a frontogenesis theory that is less restrictive than quasi-geostrophic theory and that includes the ageostrophic effects highlighted in the last section, we perform a scale analysis in a coordinate system in which the front is stationary and oriented in the y direction. Let ℓ, U and L, V be respectively length and velocity scales across and along the front. Then $\ell \ll L$ and observations show that $V \gg U$. Assuming that $D/Dt \sim U/\ell$, the ratios of the accelerations and the Coriolis forces in the x and y directions are

$$(Du/Dt)/fv \sim (U/V)^2 (V/f\ell) \text{ and } (Dv/Dt)/fu \sim V/f\ell .$$

In the long-front (y) direction the acceleration is of first-order importance

if the front is strong enough that $V/f\ell \sim 1$. However, the cross-front acceleration, Du/Dt , should be smaller than the Coriolis force in the x direction so that this force must be balanced by the pressure gradient. A more detailed scale analysis is given in Hoskins & Bretherton (1972). The implication is that v may be approximated by its geostrophic value. Then the y momentum and buoyancy equations may be written

$$Dv_g/Dt + fu_a = 0, \quad (14)$$

and

$$Db/Dt = 0. \quad (15)$$

Comparing with the quasi-geostrophic versions (6) and (7), the crucial extra ingredient is the advection by the full ageostrophic motion in the (x, z) plane, so that D/Dt is a full three-dimensional material time derivative.

This approximation, which is a two-dimensional version of the geostrophic momentum approximation introduced by Eliassen (1948), was first used by Sawyer (1956) and Eliassen (1959, 1962) to derive a more complicated version of (12). Performing an analysis identical with that used in deriving (12) but starting from (14) and (15) gives the cross-front stream-function equation:

$$N^2\psi_{xx} - 2S^2\psi_{xz} + F^2\psi_{zz} = -2Q_1, \quad (16)$$

where $N^2 = b_z$, $S^2 = b_x = fv_z$, and $F^2 = f(f + v_x)$. The operator on the left-hand side is elliptic provided the potential vorticity $q = F^2N^2 - S^4$ is positive or, equivalently, the fluid is symmetrically stable (Hoskins 1974). It can be shown from (14) and (15) plus the mass conservation and hydrostatic relations that q is conserved following a fluid particle. The forcing term in (16) is identical with that in the quasi-geostrophic version (12).

The qualitative ideas on vertical circulations in a region of frontogenesis gained from quasi-geostrophic theory and illustrated in Figure 2 need only a little modification. As indicated in Figure 3a thermal wind balance, from (14) and (15), may be shown to be maintained by gradients in w along buoyancy surfaces and by gradients in u_a along "absolute momentum" lines $X = x + v_g/f = \text{constant}$. Now it is easily seen that

$$q = f^2\partial(X, b)/\partial(x, z). \quad (17)$$

Since q is conserved on a fluid particle, as gradients in X and b increase, i.e. N^2 , S^2 , and F^2 increase, so the angles between X and b lines decrease. The ellipticity of Equation (16) becomes weaker and the boundary condition $\psi = 0$ at $z = 0$ becomes more difficult to satisfy.

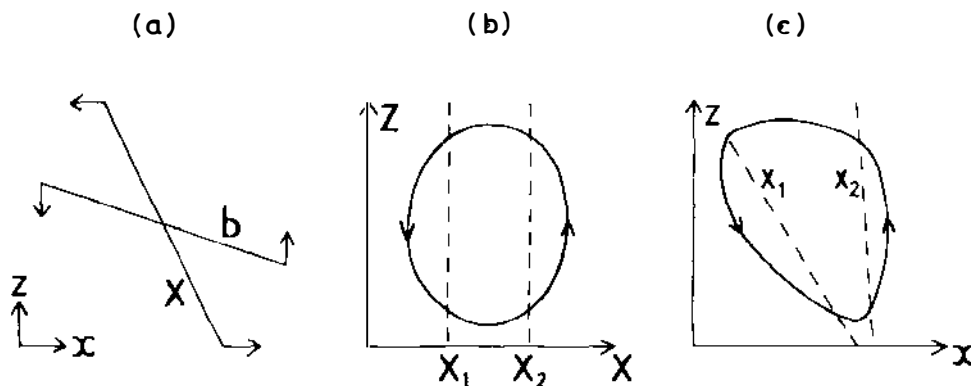


Figure 3 (a) Ageostrophic motions (indicated by arrows) which tend to restore thermal wind balance when Q_1 is positive. By analogy with (1), (3), and (4), the gradient in w along the b contour decreases b_x and the gradient in u_a along the $X = x + v_g/f$ contour increases v_x . (b) The circulation around a closed contour in the XZ plane in a region where Q_1 is positive. (c) The same circulation in the xz plane. The dashed lines are lines of constant X which are close together near the surface in a region of large vorticity.

Mathematically it is simplest to follow Eliassen (1962) and use X as independent variable instead of x which then turns (16) into

$$f^{-2}(q \psi_x)_x + f^2 \psi_{zz} = -2Q_1/J. \quad (18)$$

Here $Z = z$, and $J = \partial X/\partial x = 1 + f^{-1} \partial v_g/\partial x$ is the Jacobian of the transformation. For a closed circulation around a region where $Q_1 > 0$, the circulation must have the sense shown in Figure 3b. Transformation back to x, z coordinates tilts the ellipses along lines $X = \text{constant}$ and produces more intense flow in regions in which J is large, i.e. the relative vorticity $\xi = \partial v_g/\partial x$ is significant in comparison with f^2 . This is sketched in Figure 3c.

We now have the extra effect that quasi-geostrophic theory did not even suggest. As the frontal gradients increase in region P in Figure 2, so the ageostrophic convergence there increases. To be specific, suppose that near P , $\partial w/\partial z = \gamma \xi$ where $\gamma \sim .2$ would be not unreasonable. For a fluid particle remaining at P , infinite vorticity would be produced in a time $\ln 2/\gamma f$ after the relative vorticity reached f . Typical numbers give this time to be ~ 10 hours. In reality, of course, the approximations of no frictional processes and geostrophic long-front velocity would break down somewhat before this time.

As mentioned in the introduction, the other region of strong atmospheric frontogenesis is near the tropopause. The quasi-geostrophic arguments

²Note that $\partial u/\partial y$ is neglected in ξ consistent with the approximations made.

presented in Section 3 suggested frontogenesis on the cold side of the thermal contrast but assumed that the tropopause was rigid. To obtain a better indication of the process of upper-air frontogenesis it is necessary to consider atmospheric structure in the region of the tropopause. In terms of potential vorticity, the tropopause marks a transition from the relatively low values in the troposphere to high values in the stratosphere. Near the tropopause in a region of tropospheric temperature gradients the thermal structure is generally as shown in Figure 4. The tropopause slopes and there is a tendency for a reversed horizontal thermal gradient about it. If Q_1 is positive then the cross-frontal circulation must look approximately as indicated. The high potential vorticity in the stratosphere implies generally small vertical motion there. The effect of the circulation is to steepen the tropopause and also to make it descend near R . Large velocity and temperature gradients may be expected in the region R but a tendency to produce infinite gradients in a finite time is unlikely.

The cross-frontal circulation equation either in the form (16) or (18) has been the subject of numerous investigations. Sawyer (1956) first derived the equation in a study of frontogenesis in a prescribed deformation field. He exhibited numerical solutions for particular geostrophic fields and also assessed possible modifications due to latent-heat release. Eliassen (1959) concentrated on the forcing of (16) by a latent-heat release term $-H_x$ where H is a term added to the right-hand side of (15) and also on an Ekman pumping boundary condition. Eliassen (1962) exhibited for the first time the full forcing term Q_1 and also the transformation to the normal form (18). More recently, Shapiro (1981) has solved the equation for

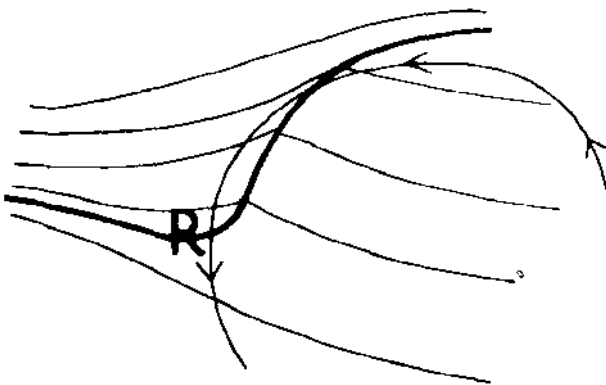


Figure 4 The ageostrophic circulation in the region of the tropopause (thick line) assuming Q_1 is positive. Temperature contours are marked by continuous lines. In three-dimensional models, as discussed below, it is often found that Q_1 is negative near R , which forces the descent to be concentrated and to the right of R .

geostrophic fields taken from observed and simulated frontogenesis cases. He has also incorporated a parameterization of clear-air turbulence into the forcing term.

Time-Dependent Models

GENERAL COMMENTS Simple time-dependent models of frontogenesis have also been formulated in terms of potential vorticity q , buoyancy b , and coordinate X . We recall that q is a conservative quantity that is proportional to the Jacobian of X and b with respect to x and z as shown in (17). From its definition, $X = x + \phi_x/f^2$ and also $b = \phi_z$. As Gill (1981) pointed out, the thermal wind relation can be written

$$\partial(b, z)/\partial(X, x) = -f^2. \quad (19)$$

Thus the potential vorticity definition and the thermal wind relation both reduce to linear form if X and z or x and b are taken as independent variables. Buoyancy (or isentropic) coordinates x and b may often be useful for describing interior motions (Shapiro 1975) but where bounding surfaces are at constant z it is more convenient to use X and z . The boundary condition on such a surface is then that b is conserved in horizontal motion. To see how X changes on a fluid particle we use the y equation of motion (14) to obtain

$$DX/Dt = u_g. \quad (20)$$

Thus in X space the horizontal motion is geostrophic.

For the case where the frontogenesis is forced by a simple deformation $u = -\alpha x$, $v = \alpha y$, it is most convenient, following Hoskins & Bretherton (1972), to return to the full equations and set

$$u = -\alpha x + u', \quad v = \alpha y' + v', \\ \phi = f\alpha xy - 1/2 \alpha^2 (x^2 + y^2)$$

Scale analysis then suggests that v' is approximately the geostrophic value ϕ'_x/f . It is then consistent to consider a model in which all the primed variables are independent of y . Defining $X = x + v'/f$ all the above relations are valid for this problem except that (20) is replaced by

$$DX/Dt = -\alpha X. \quad (21)$$

Thus $X = X_0 e^{-\alpha t}$ on a fluid particle.

ZERO POTENTIAL VORTICITY DEFORMATION MODEL The simplest time-dependent frontogenesis model that yields realistic results is obtained by considering the simple deformation acting on a fluid of zero potential vorticity and bounded by surfaces at $z = \pm H/2$. From (17), at any

instant b must be a function of X only. Since b is conserved and the behavior of X is given by (21), we find that

$$b = F(X e^{at}). \quad (22)$$

From the thermal wind equation (19),

$$(\partial z / \partial x)|_{b=\text{const}} = -f^2 / b_X. \quad (23)$$

Thus lines on which b and X are constant are straight and of known slope at time t if F is known.

Mass conservation gives that at $z = 0$ the line must be at the same position as it would have been if it had moved with the deformation velocity alone, i.e. $X = x$. Thus on an X, b line,

$$x = X - f^{-2} z b_X. \quad (24)$$

Therefore

$$v' = f(X - x) = f^{-1} z b_X. \quad (25)$$

The vertical component of absolute vorticity is

$$\zeta = f \partial X / \partial x = f(1 - f^{-2} z b_{XX})^{-1}. \quad (26)$$

Specification of the geostrophic fields at an initial instant gives the function F in (22). At later times the solution is given by (22), (24), and (25). Time t has become a simple parameter in the solution.

A specific solution is shown in Hoskins & Bretherton (1972). Here we will note that the solution quite generally supports the inferences made above. In particular, in the lower half of the fluid the frontogenesis proceeds most rapidly at the lower boundary on the warm side where θ_{XX} is most negative. There infinite gradients are predicted in a finite time. In fact, it is easily shown that on the lower boundary the parameter γ giving the ratio between the ageostrophic convergence and the vorticity is $2\alpha/f$, so that the time scale for infinite vorticity is α^{-1} .

Finally, we note that this solution gives a good indication of the range of validity of our geostrophic approximation and neglect of mixing processes. The former is found to be consistent if $\zeta/f \ll (2\alpha/f)^{-2} \sim 25$. For zero potential vorticity, the Richardson number is equal to f/ζ so that one may expect mixing processes to be important before $\zeta = 10f$.

OTHER SIMPLE MODELS Multiplying (19) by the Jacobian of X and x with respect to X and Z shows that thermal wind balance takes the same form in X, Z coordinates as in real space. The potential function

$$\Phi = \phi + 1/2 v_g^2 \quad (27)$$

then gives

$$f v_g = \Phi_X, \quad b = \Phi_Z. \quad (28)$$

The Jacobian of the transformation to X coordinates is

$$J = \zeta/f = (1 - \Phi_{xx}/f^2)^{-1} \quad (29)$$

and (17) gives

$$f^{-2} \Phi_{xx} + f^2 q^{-1} \Phi_{zz} = 1. \quad (30)$$

The next simplest frontogenesis model after the deformation model with a zero potential vorticity fluid is that with a uniform potential vorticity fluid. On rigid horizontal boundaries, b is again given for all time by (22). Thus the total geostrophic solution at any subsequent time is given by a solution of the simple second-order elliptic equation (30) with Φ_z specified on horizontal boundaries and suitable conditions on Φ at large $|X|$ away from the region of interest. Such solutions have been discussed in detail in Hoskins (1971), and compared with observed frontogenesis by Blumen (1980). There are no substantial differences from the zero potential vorticity solution. Again, infinite gradients are predicted in a finite time $O(\alpha^{-1})$. Determination of the ageostrophic circulation is not necessary for solution of the time-dependent problem but is a simple matter from (18) with the right-hand side $-2\alpha b_x$.

A uniform potential vorticity model in which the frontogenesis is initiated by the horizontal shear mechanism of Figure 1*b* is given by the two-dimensional Eady problem (Eady 1949). The basic state is a uniform negative meridional buoyancy gradient \bar{b}_y in thermal wind balance with u_g increasing linearly with height. Perturbations of the form $(a \cosh kZ \cos kX + b \sinh kZ \sin kX)$ trivially satisfy the interior equation (30) and substitution in the buoyancy-conservation equation on the two horizontal boundaries shows that exponential growth is possible. The growing baroclinic wave again contains frontal gradients on the boundaries which tend to become infinite in a finite time $O(N/\bar{b}_y)$. This problem was first solved numerically by Williams (1967) without the approximation of the geostrophy of v . The later analytical solution (Hoskins & Bretherton 1972) using this approximation showed good agreement.

It is worth noting that both the uniform potential vorticity solutions for v_g and b are mathematically identical with quasi-geostrophic solutions except that these values are obtained in the distorted X space. The simple interpretation from (14) is that to accelerate to a geostrophic velocity V in the y direction, a particle must receive an ageostrophic displacement $-V/f$ in the x direction. This displacement is not included in quasi-geostrophic theory. It implies a strengthening of positive relative vorticity and weakening of negative vorticity such that relative vorticities of $-f$, 0 , $f/2$, and f in a quasi-geostrophic solution become $-f/2$, 0 , f , and ∞ .

The next level of complexity is achieved by proceeding to a model in which the deformation acts on a fluid with two regions of uniform potential vorticity separated by an interface. In the two regions (30) holds and on

rigid boundaries (22) again gives Φ_z . On the interior boundary, Φ_z is also given by (22) but the position of the boundary is determined such that Φ_x is continuous. The solution may be determined numerically using iterative techniques (Hoskins & Bretherton 1972). In the atmospheric case the interest is in representing frontogenesis near the tropopause, which is an interface between high potential vorticity stratospheric air and low potential vorticity tropospheric air. Solutions exhibited in Hoskins (1971, 1972) show the descent of a narrow tongue of stratospheric air and the formation of large gradients at the base of the tongue.

MacVean & Woods (1980) have studied an oceanic example of a low-stratification "well-mixed" layer above a higher potential vorticity layer and shown the frontogenesis and distortion of the interface. One extra ingredient highlighted by their paper is that oceanic buoyancy depends on temperature and salinity. Although the theory suggests that the horizontal length scale of the buoyancy field in the interior does not fall below the radius of deformation, a sharp front in temperature and salinity is possible. This is illustrated in Figure 5. There is, however, no tendency to form infinite interior gradients in a finite time.

5. THREE-DIMENSIONAL SEMI-GEOSTROPHIC THEORY

Introduction

The two-dimensional frontogenesis models show the essential nature of the dynamics but only within the imposed large-scale geostrophic frame-

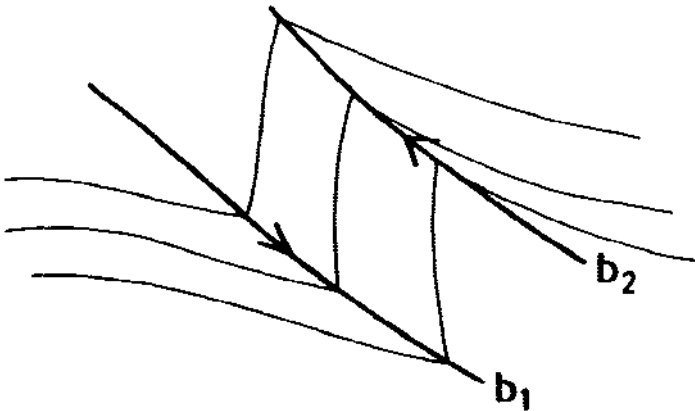


Figure 5 The interior situation during frontogenesis when buoyancy depends on more than one conservative quantity, e.g. temperature and salinity. The geostrophic motion tends to make the total velocity lie along buoyancy contours b_1 , b_2 so that increased gradients are not formed. However, gradients of any other conservative quantity (light contours) increase indefinitely.

work. The next stage is to study the formation of fronts in growing three-dimensional baroclinic waves. The numerical integration of the primitive equations by Arakawa (1962), Edlmann (1963), Eliassen & Raustein (1970), Mudrick (1974), and others indicates that such growing waves do indeed form surface fronts though the intensity of the process is limited by numerical resolution. Shapiro (1975) and Hoskins & Draghici (1977) have used isentropic coordinates to simulate upper-tropospheric frontogenesis. However, in order to extend the understanding of the processes involved from two to three dimensions we shall consider a three-dimensional theory which in a two-dimensional situation reduces to the previous theory.

Following Eliassen (1948), Fjortoft (1962), and Hoskins (1975) it is assumed that the time scale for change in velocity following a fluid particle is much larger than $f^{-1} \sim 3 h$. Now the exact, horizontal, Boussinesq vector momentum equation may be written

$$\mathbf{v} = \mathbf{v}_g + \mathbf{k} \wedge f^{-1} D\mathbf{v}/Dt . \quad (31)$$

Using this expression to substitute for \mathbf{v} in the last term gives

$$\mathbf{v} = \mathbf{v}_g + \mathbf{k} \wedge f^{-1} D\mathbf{v}_g/Dt - f^{-2} D^2\mathbf{v}/Dt^2 . \quad (32)$$

Consistent with the above assumption, the last term is neglected. This is called the geostrophic momentum approximation because the momentum equation becomes

$$D\mathbf{v}_g/Dt + f\mathbf{k} \wedge \mathbf{v} + \nabla\phi = 0 . \quad (33)$$

The ageostrophic motion is retained in the advection but not in the momentum. The advection of buoyancy is also by the full (geostrophic plus ageostrophic) flow.

Like the full Boussinesq equations, the modified set conserves buoyancy, has a full energy equation, a three-dimensional vorticity equation, and an Ertel potential vorticity conservation equation. As in the two-dimensional case, the equations are most easily considered by making a transformation to "geostrophic" coordinates:

$$X = x + v_g/f, Y = y - u_g/f .$$

Some interesting comments on this coordinate transformation have been made by Blumen (1981). As described in Hoskins (1975) a potential function

$$\Phi = \phi + 1/2(u_g^2 + v_g^2) \quad (34)$$

has derivatives in the transformed space giving the geostrophic velocities and buoyancy. The conservation of buoyancy and potential vorticity are

$$Db/Dt = 0 \quad (35)$$

$$\text{and } Dq/Dt = 0, \quad (36)$$

where the expression for the full material time derivative in geostrophic coordinates is $D/Dt = \partial/\partial T - f^{-1} \Phi_Y \partial/\partial X + f^{-1} \Phi_X \partial/\partial Y + w \partial/\partial Z$.

Making one further approximation consistent with the original assumption, Φ and the potential vorticity q are related by the elliptic equation

$$f^{-2}(\Phi_{XX} + \Phi_{YY}) + f^2 q^{-1} \Phi_{ZZ} = 1. \quad (37)$$

Given suitable lateral boundary conditions, numerical solution is possible using (36) to predict q , (35) to predict $b = \Phi_Z$ on horizontal boundaries, and (37) to obtain values of Φ everywhere. The vertical velocity, w , which is required in (36), may be obtained by consistency of the predictions of (35) and (36) in the interior of the fluid. Alternatively, as suggested in Hoskins & Draghici (1977), it can be obtained from an elliptic equation that is the analogue of the cross-frontal circulation equation (18).

This set of equations, known as the semi-geostrophic equations, is clearly an extension to three dimensions of the two-dimensional theory given in particular by (27)–(30). On the large scale they are certainly as accurate as the quasi-geostrophic equations but, unlike them, are able to represent the vertical advection of a region of large gradients in potential vorticity, e.g. the tropopause, and the dynamics of frontogenesis. McWilliams & Gent (1980) have discussed in great detail a variety of theories whose accuracy is greater than that of quasi-geostrophic theory. There is little present knowledge about the practical usefulness of the other possibilities raised.

Uniform Potential Vorticity Models

If the potential vorticity is initially uniform, then it remains uniform for all time. Thus (36) is trivial and w is not required. Time dependence enters only through the buoyancy equation (35) with $w = 0$ on horizontal boundaries. Solution proceeds by time marching the boundary equations for Φ_Z and solving the interior equation (37) at each time step.

The source of the energy for baroclinic instability is the potential energy associated with the horizontal temperature contrast and its attendant vertical shear in the horizontal wind. Various basic states $\Phi(Y, Z)$ have been used in different papers. The Eady model has a uniform buoyancy gradient:

$$\bar{\Phi} = N^2 Z^2/2 - fUYZ/H.$$

Other flows in Hoskins & West (1979) are modifications of this but always such that

$$f^{-2} \bar{\Phi}_{YY} + N^{-2} \bar{\Phi}_{ZZ} = 1,$$

where $N^2 = q/f^2$ is constant. The fluid is considered to be doubly periodic in the horizontal. The next step is to study the linear stability of the flow

and then to initiate an integration of the semi-geostrophic equations using as initial conditions Φ plus a small-amplitude unstable normal mode.

The Eady mode independent of Y is a solution of the nonlinear equations and has been discussed above and illustrated in Hoskins & Bretherton (1972) and Hoskins & West (1979). Eady modes with a finite periodicity in Y have been discussed in Hoskins (1976). These solutions did not produce very realistic frontogenesis. In Hoskins & West (1979) the first flows considered were only minor modifications to the Eady flow in which buoyancy gradients were concentrated more in the center of the region of interest. The most unstable modes were modifications of the two-dimensional Eady modes. These solutions exhibited more realistic frontogenesis.

Here we shall comment only on two particular solutions in Hoskins & West (1979). The first corresponds to a basic flow that is zero at $z = 0$ rising to $U(1 + \cos \ell Y)/2$ at the top. At day 6.3 of the integration the situation at the surface is as shown in Figure 6. A strong surface cold front has formed, there being a tendency to form infinite gradients in velocity and buoyancy in a finite time. A weaker warm front has just started to appear to the northeast of the low. Both fronts are on the "warm side" of the contrast consistent with the two-dimensional theory. As discussed in much more detail in Hoskins & West (1979) the crucial factors to consider are

1. the frontogenetic nature of the large-scale geostrophic motion as shown by the deformation or the vector \mathbf{Q} [see(5)],
2. the trajectories of fluid particles relative to the system.

The cold front region, particularly towards the low pressure, is a frontogenetic region. There the \mathbf{Q} vectors point almost directly towards the warm air (Hoskins & Pedder 1980). Fluid particles in a small-amplitude mode move westwards through the system. As the amplitude increases so particles slow down equatorward of the low and move along the cold frontal region in the manner indicated. The warm frontal region is also frontogenetic but particles move quickly through it and around the low. The warm front only really develops when the velocities in the eddy are large enough that fluid particles begin to move northwards and eastwards relative to the system as shown.

The second case to be discussed is for a basic flow $-.15 U \cos \ell y$ at the lower surface rising to $.85 U$ at the top. In this case the most unstable linear mode tilts in the horizontal as if advected by the low-level flow. At day 5.5 the surface development is as shown in Figure 7. There is this time no real cold front (except perhaps the rather unrealistic region on the poleward side of the low) but a strong warm front in a different position from that of the weak warm front in the previous example. It can be shown

from the \mathbf{Q} vectors that the previous cold frontal position is no longer frontogenetic but that the new warm frontal position is. The trajectories of fluid particles are such that they move along the developing warm front towards the low-pressure center.

These two examples indicate the possibility in a developing baroclinic wave of either a primary cold front and a secondary warm front (type A) or a primary warm front (type B). The nonlinear frontogenetic tendency to form infinite gradients in a finite time is just as described in the two-dimensional theory. The primary cold front and warm front have very different characteristics. In particular the former has a relatively steep slope and is associated with significant positive vorticity through the depth whilst the latter is relatively shallow in slope and in the depth of positive vorticity. It is shown in Hoskins & Heckley (1981) that these quite realistic differences are associated with the forward tilt with height of the temper-

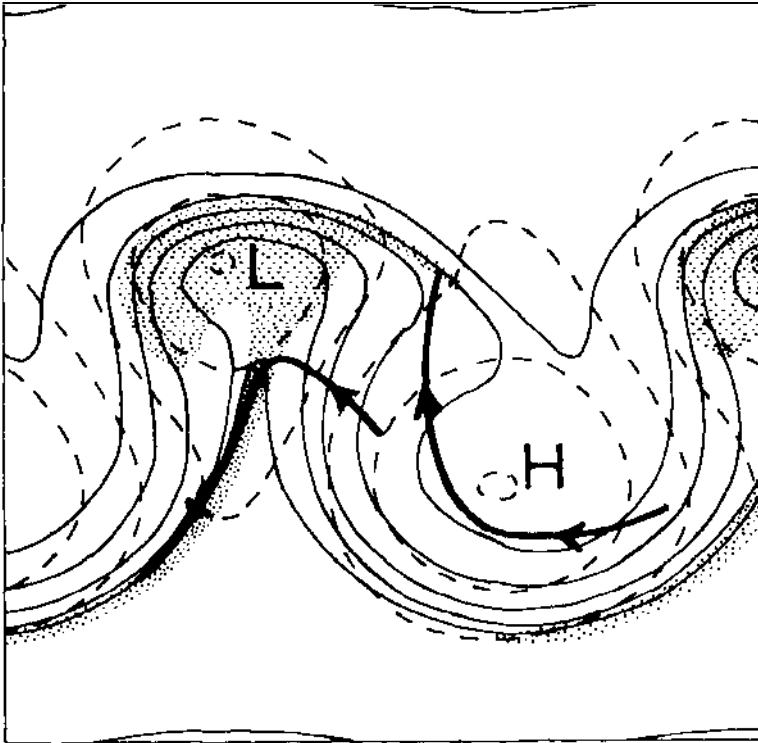


Figure 6 Surface map at day 6.3 for the first case discussed in the text. Temperature contours every 4 K are continuous lines, ϕ contours dashed lines, and the region of relative vorticity larger than $f/2$ is shaded. The relative vorticity in the cold front region has a maximum of $5f$. The bold lines indicate two trajectories relative to the system from day 3.

ature wave in a growing disturbance. The theoretical work of Gidel (1978) should also be mentioned. He attributed some of the differences between warm and cold fronts to the opposite sign of the thermal gradient along the two sorts of front.

Non-Uniform Potential Vorticity Models

Full semi-geostrophic integrations have been described in Heckley (1980). In particular some models have included an explicit stratosphere. The surface frontogenesis is not altered but upper troposphere frontogenesis can be simulated. One point of agreement with Shapiro (1981) and numerous observational studies is that just in the region of the upper-air front the Q vectors point towards colder air suggesting the possibility of an indirect circulation with cold air rising and warm air descending. However, in the context of the generally direct forcing in the wave, the negative geostrophic frontogenesis function locally means that descent is strongest on the warm side of the descending stratospheric tongue (see Figure 4).

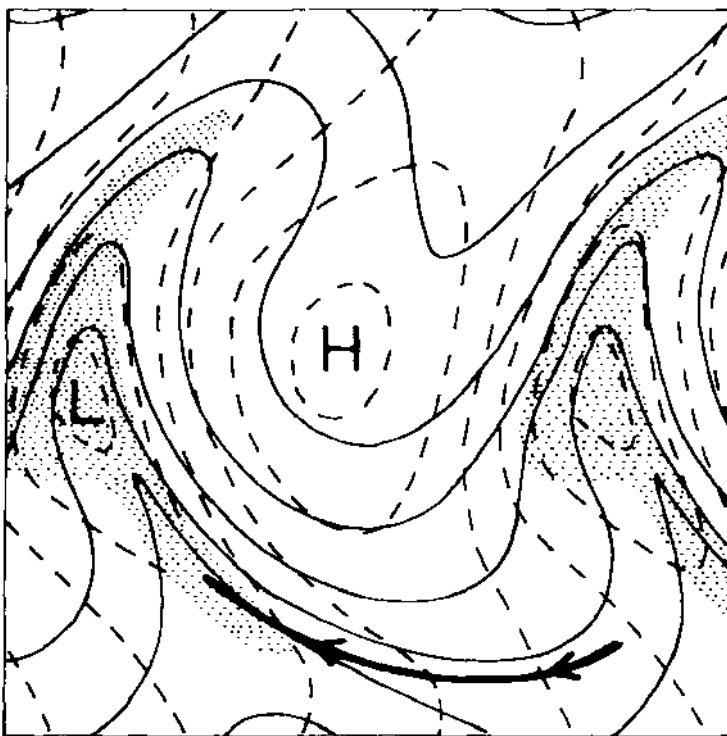


Figure 7 Surface map at day 5.5 for the second case discussed in the text. Conventions are as in Figure 6 except that the temperature contour interval is 8 K.

6. SUMMARY

The analysis described in this paper has indicated why contrasts in velocity and buoyancy in a rapidly rotating fluid tend to be concentrated in frontal regions. The sharpness of these regions depends on the strength of the mixing processes which eventually must balance the frontogenetic mechanism. In frontogenesis all scales are linked directly as discussed by Blumen (1978a, b). If mixing is weak enough that sharp fronts may form, an energy spectrum behaving like a $-8/3$ power of the wavenumber is predicted by semi-geostrophic theory (Andrews & Hoskins 1978).

For a more realistic comparison with frontogenesis in the Earth's atmosphere the modifying effects of various additional physical processes may be considered. Compressibility effects may be added to the theory in a simple manner (Hoskins & Bretherton 1972) and produce only qualitative changes. The feedback on frontogenesis of latent-heat release in the rising warm air may be expected to quicken the process (Orlanski & Ross 1978). Bennetts & Hoskins (1979) suggested that it could also make the effective potential vorticity negative, thereby rendering (16) hyperbolic and the fluid symmetrically unstable. This could be the reason for the frequently banded structure of the precipitation in frontal regions. The interactions of frontal regions with the surface boundary layer and with topographic features are important and not well understood. One example of the latter has been highlighted recently by Baines (1981). As mentioned above, Shapiro (1981) has discussed the effects of turbulent fluxes in the free atmosphere. Williams (1974) exhibited a numerical model in which mixing processes eventually balanced the frontogenetic tendency to produce a steady-state front.

Another important area is that of the stability of fronts. The forecasting of the development of waves on atmospheric fronts is based on poorly understood empirical rules. Some theoretical work has been performed by Eliassen (1960), Orlanski (1968), Duffy (1976), and Grotjhan (1979).

As discussed in this paper, much progress has been made on the understanding of why fronts form, but our knowledge of the interplay of all the processes occurring in frontal regions is still in its infancy.

ACKNOWLEDGMENTS

The author is very grateful to Dr. David Andrews and Dr. Malcolm MacVean for their speedy and thorough reviews of the first version of this paper.

Literature Cited

- Andrews, D. G., Hoskins, B. J. 1978. Energy spectra predicted by semi-geostrophic theories of frontogenesis. *J. Atmos. Sci.* 35: 509-12
- Arakawa, A. 1962. Non-geostrophic effects in the baroclinic prognostic equations. *Proc. Int. Symp. Numerical Weather Prediction, Tokyo*, pp. 161-75

- Baines, P. G. 1981. The dynamics of the Southerly Buster. *Aust. Meteorol. Mag.* In press
- Bennetts, D. A., Hoskins, B. J. 1979. Conditional symmetric instability—a possible explanation for frontal rainbands. *Q. J. R. Meteorol. Soc.* 105:945–62
- Bergeron, T. 1928. Über die dreidimensional verknüpfende Wetteranalyse I. *Geofys. Publikasjoner* 5(No. 6):1–111
- Blumen, W. 1978a. Uniform potential vorticity flow: Part I. Theory of wave interactions and two dimensional turbulence. *J. Atmos. Sci.* 35:774–83
- Blumen, W. 1978b. Uniform potential vorticity flow: Part II. A model of wave interactions. *J. Atmos. Sci.* 35:784–89
- Blumen, W. 1980. A comparison between the Hoskins-Bretherton model of frontogenesis and the analysis of an intense surface frontal zone. *J. Atmos. Sci.* 37:64–77
- Blumen, W. 1981. The geostrophic coordinate transformation. *J. Atmos. Sci.* 38:1100–5
- Charney, J. G. 1947. The dynamics of long waves in a baroclinic westerly current. *J. Meteorol.* 4:135–63
- Duffy, D. G. 1976. The application of the semi-geostrophic equations to the frontal instability problem. *J. Atmos. Sci.* 33:2322–37
- Eady, E. T. 1949. Long waves and cyclone waves. *Tellus* 1:33–52
- Edelmann, W. 1963. On the behaviour of disturbances in a baroclinic channel. Summary Rep. No. 2, *Research in Objective Weather Forecasting*, Part F. Contract AF61(052)-373. Deut. Wetter., Offenbach. 35 pp.
- Eliassen, E. 1960. On the initial development of frontal waves. *Publ. Danske Met. Inst.* 13. 107 pp.
- Eliassen, A. 1948. The quasi-static equations of motion. *Geofys. Publikasjoner* 17, No. 3
- Eliassen, A. 1959. On the formation of fronts in the atmosphere. *The Atmosphere and the Sea in Motion*, pp. 277–87. NY: Rockefeller Institute Press
- Eliassen, A. 1962. On the vertical circulation in frontal zones. *Geofys. Publikasjoner* 24 (No. 4):147–60
- Eliassen, A., Raustein, E. 1970. A numerical integration experiment with a six-level atmospheric model with isentropic information surfaces. *Meteorol. Ann.* 5: 429–49
- Faller, A. J. 1956. A demonstration of fronts and frontal waves in atmospheric models. *J. Meteorol.* 13:1–4
- Fjortoft, R. 1962. On the integration of a system of geostrophically balanced prognostic equations. *Proc. Int. Symp. Numerical Weather Prediction, Tokyo*, pp. 153–59
- Fultz, D. 1952. On the possibility of experimental models of the polar front wave. *J. Meteorol.* 9:379–84
- Gidel, L. T. 1978. Simulation of the differences and similarities of warm and cold surface frontogenesis. *J. Geophys. Res.* 83:915–28
- Gill, A. E. 1981. Homogeneous intrusion in a rotating stratified fluid. *J. Fluid Mech.* 103:275–95
- Grotjhan, R. 1979. Cyclone development along weak thermal fronts. *J. Atmos. Sci.* 36:2049–74
- Heckley, W. A. 1980. *Frontogenesis*. PhD thesis. Univ. Reading. 209 pp.
- Hoskins, B. J. 1971. Atmospheric frontogenesis: some solutions. *Q. J. R. Meteorol. Soc.* 97:139–53
- Hoskins, B. J. 1972. Non-Boussinesq effects and further development in a model of upper tropospheric frontogenesis. *Q. J. R. Meteorol. Soc.* 98:532–41
- Hoskins, B. J. 1974. The role of potential vorticity in symmetric stability and instability. *Q. J. R. Meteorol. Soc.* 100: 480–82
- Hoskins, B. J. 1975. The geostrophic momentum approximation and the semi-geostrophic equations. *J. Atmos. Sci.* 32: 233–42
- Hoskins, B. J. 1976. Baroclinic waves and frontogenesis. Part I: Introduction and Eady waves. *Q. J. R. Meteorol. Soc.* 102: 103–22
- Hoskins, B. J., Bretherton, F. P. 1972. Atmospheric frontogenesis models: mathematical formulation and solution. *J. Atmos. Sci.* 29:11–37
- Hoskins, B. J., Draghici, I. 1977. The forcing of ageostrophic motion according to the semi-geostrophic equations and in an isentropic coordinate model. *J. Atmos. Sci.* 34:1859–67
- Hoskins, B. J., Heckley, W. A. 1981. Cold and warm fronts in baroclinic waves. *Q. J. R. Meteorol. Soc.* 107:79–90
- Hoskins, B. J., Pedder, M. A. 1980. The diagnosis of middle latitude synoptic development. *Q. J. R. Meteorol. Soc.* 106:707–19
- Hoskins, B. J., West, N. V. 1979. Baroclinic waves and frontogenesis. Part II: Uniform potential vorticity jet flows—cold and warm fronts. *J. Atmos. Sci.* 36:1663–80
- Katz, E. J. 1969. Further study of a front in the Sargasso Sea. *Tellus* 21:259–69
- MacVean, M. K., Woods, J. D. 1980. Redistribution of scalars during upper ocean frontogenesis: a numerical model. *Q. J. R. Meteorol. Soc.* 106:293–312

- McWilliams, J. C., Gent, P. R. 1980. Intermediate models of planetary circulations in the atmosphere and ocean. *J. Atmos. Sci.* 37:1657-78
- Miller, J. E. 1948. On the concept of frontogenesis. *J. Meteorol.* 5:169-71
- Mudrick, S. E. 1974. A numerical study of frontogenesis. *J. Atmos. Sci.* 31:869-92
- Orlanski, I. 1968. Instability of frontal waves. *J. Atmos. Sci.* 25:178-200
- Orlanski, I., Ross, B. B. 1978. The circulation associated with a cold front. Part II: Moist case. *J. Atmos. Sci.* 35:445-65
- Pedlosky, J. 1979. *Geophysical Fluid Dynamics*. NY: Springer. 624 pp.
- Reed, R. J., Danielsen, E. F. 1959. Fronts in the vicinity of the tropopause. *Arch. Meteorol. Geophys. Bioklim.* A11:1-17
- Sawyer, J. S. 1956. The vertical circulation at meteorological fronts and its relation to frontogenesis. *Proc. R. Soc. London Ser. A* 234:346-62
- Shapiro, M. A. 1975. Simulation of upper-level frontogenesis with a 20-level isentropic coordinate primitive equation model. *Mon. Weather Rev.* 103:591-604
- Shapiro, M. A. 1981. Frontogenesis and geostrophically forced secondary circulations in the vicinity of jet stream-frontal zone systems. *J. Atmos. Sci.* 38:954-73
- Stone, P. H. 1966. Frontogenesis by horizontal wind deformation fields. *J. Atmos. Sci.* 23:455-65
- Voorhis, A. D., Hersey, J. B. 1964. Oceanic thermal fronts in the Sargasso Sea. *J. Geophys. Res.* 69:3809-14
- Williams, R. T. 1967. Atmospheric frontogenesis: a numerical experiment. *J. Atmos. Sci.* 24:627-41
- Williams, R. T. 1968. A note on quasi-geostrophic frontogenesis. *J. Atmos. Sci.* 25:1157-59
- Williams, R. T. 1974. Numerical simulation of steady-state fronts. *J. Atmos. Sci.* 31:1286-96
- Williams, R. T., Plotkin, J. 1968. Quasi-geostrophic frontogenesis. *J. Atmos. Sci.* 25:201-6



CONTENTS

| | |
|--|-----|
| VILHELM BJERKNES AND HIS STUDENTS, <i>Arnt Eliassen</i> | 1 |
| SEDIMENT RIPPLES AND DUNES, <i>Frank Engelund and Jørgen Fredsøe</i> | 13 |
| STRONGLY NONLINEAR WAVES, <i>L. W. Schwartz and J. D. Fenton</i> | 39 |
| TOPOLOGY OF THREE-DIMENSIONAL SEPARATED FLOWS, <i>Murray Tobak and David J. Peake</i> | 61 |
| DYNAMICS OF GLACIERS AND LARGE ICE MASSES, <i>Kolumban Hutter</i> | 87 |
| THE MATHEMATICAL THEORY OF FRONTOGENESIS, <i>B. J. Hoskins</i> | 131 |
| DYNAMICS OF LAKES, RESERVOIRS, AND COOLING PONDS, <i>Jörg Imberger and Paul F. Hamblin</i> | 153 |
| TURBULENT JETS AND PLUMES, <i>E. J. List</i> | 189 |
| GRAVITY CURRENTS IN THE LABORATORY, ATMOSPHERE, AND OCEAN, <i>John E. Simpson</i> | 213 |
| THE FLUID DYNAMICS OF HEART VALVES: EXPERIMENTAL, THEORETICAL, AND COMPUTATIONAL METHODS, <i>Charles S. Peskin</i> | 235 |
| THE COMPUTATION OF TRANSONIC POTENTIAL FLOWS, <i>David A. Caughey</i> | 261 |
| UNSTEADY AIRFOILS, <i>W. J. McCroskey</i> | 285 |
| LOW-GRAVITY FLUID FLOWS, <i>Simon Ostrach</i> | 313 |
| THE STRANGE ATTRACTOR THEORY OF TURBULENCE, <i>Oscar E. Lanford III</i> | 347 |
| DYNAMICS OF OIL GANGLIA DURING IMMISCIBLE DISPLACEMENT IN WATER-WET POROUS MEDIA, <i>A. C. Payatakes</i> | 365 |
| NUMERICAL METHODS IN FREE-SURFACE FLOWS, <i>Ronald W. Yeung</i> | 395 |
| INDEXES | |
| Author Index | 443 |
| Cumulative Index of Contributing Authors, Volumes 10–14 | 451 |
| Cumulative Index of Chapter Titles, Volumes 10–14 | 453 |